[CANCER RESEARCH 64, 7995–8001, November 1, 2004]

A Prostate-Specific Membrane Antigen-Targeted Monoclonal Antibody–Chemotherapeutic Conjugate Designed for the Treatment of Prostate Cancer

Michael D. Henry,[1] Shenghua Wen,[1] Matthew D. Silva,[2] Sudeep Chandra,[2] Mark Milton,[3] and Peter J. Worland[1]

Departments of [1]Cancer Pharmacology, [2]Imaging Sciences and [3]Drug Safety and Disposition, Millennium Pharmaceuticals, Inc., Cambridge, Massachusetts

ABSTRACT

MLN2704 is an antibody-chemotherapeutic conjugate designed to target prostate-specific membrane antigen (PSMA). PSMA is a transmembrane receptor whose expression is largely restricted to prostatic epithelium and prostate cancer cells with its expression level increasing during the progression of malignancy. MLN2704 consists of a de-immunized, monoclonal antibody that is specific for PSMA conjugated to drug maytansinoid 1 (DM1), a microtubule-depolymerizing compound. After antibody binding to PSMA and the subsequent cellular internalization of this complex, DM1 is released leading to cell death. MLN2704 has an approximate half-life of 39 hours in *scid* mice bearing CWR22 tumor tissue, and the antibody effectively penetrates xenograft tumor tissue. Optimization of dosage and schedule of MLN2704 administration defined interdependency between these conditions that maximized efficacy with no apparent toxicity. Tumor growth delays of ~100 days could be achieved on the optimized schedule of one dose of 60 mg/kg MLN2704 every 14 days for five doses (q14d×5). The unconjugated antibody (MLN591) demonstrated essentially no antitumor activity and DM1 alone or a non-PSMA targeted antibody–DM1 conjugate was only weakly active. Furthermore, we show that MLN2704 is active in a novel model of osteoblastic prostate cancer metastasis.

INTRODUCTION

Cytotoxic agents coupled to monoclonal antibodies, or immunoconjugates, specifically targeting tumor antigens, are an important class of anticancer agents currently both in clinical development and available as approved drugs (1). The promise of immunoconjugates lies in the possibility that they may improve the therapeutic index for a particular cytotoxic agent (chemotherapeutic, toxin, or radionuclide) by targeting that agent to the tumor while simultaneously reducing systemic exposure. Prostate-specific membrane antigen (PSMA), a homodimeric type II integral membrane protein that has two enzymatic activities (folate hydrolase and NAALADase) is an ideal target for this approach (2, 3). The expression of PSMA predominates in prostatic epithelial cells and is up-regulated throughout the course of prostate cancer progression (4, 5). Its expression has also been documented in the neovasculature of other types of solid tumors (6). PSMA is a highly abundant receptor on prostate cancer cells and, via clathrin-coated pits, is constitutively internalized, a process that may be accelerated by specific antibody binding (7). Because of these properties, PSMA has been the target of a variety of therapeutic approaches in prostate cancer including the delivery of immunoconjugates, immunotherapy, and prodrugs (8).

Our approach to targeting PSMA uses the deimmunized anti-PSMA, monoclonal antibody MLN591. MLN591 is derived from the murine anti-human PSMA monoclonal antibody J591, specific for the extracellular domain of PSMA (6). The antibody variable domains of J591 were first deimmunized by site-directed mutagenesis of putative T-cell reactive epitopes and were then fused to a human IgG1 backbone to further reduce the immunogenic potential of this antibody in humans (9). MLN2704 (Fig. 1) was constructed by the conjugation of drug maytansinoid 1 (DM1) to MLN591 with previously described methods through thiopentanoate linker modification of the antibody, resulting in an immunoconjugate that contains, on average, three-to-four DM1 molecules per antibody molecule (10, 11). DM1, a potent microtubule-depolymerizing drug, is an analog of maytansine, a naturally occurring ansa macrolide (11). Maytansine was evaluated as a chemotherapeutic in the 1970s and 1980s but was not developed further because of dose-limiting toxicity (12). Thus, MLN2704 is designed to bind to PSMA on the surface of prostate cancer cells and to release active DM1 on cellular internalization via reduction of the sulfhydryl linkage.

We have demonstrated that MLN2704 safely delivers dose- and schedule-dependent efficacy that is not observed with either its antibody or chemotherapeutic constituents alone in the CWR22 xenograft model of prostate cancer. We have also described the plasma pharmacokinetics of MLN2704 and observed the appearance of deconjugated MLN591 concomitant with the clearance of MLN2704. Analysis of subcutaneous xenograft tumor tissue indicates that MLN2704 is able to penetrate the targeted tissue at the first time sampled (6 hours), with the human IgG portion remaining detectable throughout the tumor by 72 hours. Finally, we show that MLN2704 demonstrates antitumor activity in a novel model of osteoblastic prostate bone metastasis. Together these preclinical data support the rationale for clinical development of MLN2704.

MATERIALS AND METHODS

Monoclonal Antibody Conjugates and Other Test Articles. MLN2704 was prepared under Good Manufacturing Practice conditions at ImmunoGen (Norwood, Massachusetts) with previously described methods (10, 11), MLN591 was obtained from Lonza (Slough, United Kingdom) and DM1 and maytansine were obtained from ImmunoGen. A humanized anti-human CCR2-DM1 was prepared at Millennium Pharmaceuticals, (Cambridge, MA) in a manner similar to MLN2704.

Xenografts and Tumor Growth Analysis. All of the animal procedures were performed in accordance with Institutional Animal Care and Use Committee guidelines. CWR22 tumors were established as described in male, 5- to 8-week-old C.B-17 *scid* mice (Taconic, Germantown, NY; ref. 13). Beginning at day 7 after implantation, and continuing daily thereafter, the tumors were measured in two dimensions by Vernier calipers, and mouse body weight was measured. Tumor volume was calculated with the following formula: tumor volume = $0.5 (L \times W^2)$, where L = length, and W = width. Tumors were allowed to grow ~3 weeks until such time as animals could be randomly assigned into study groups ($n = 8$) with mean tumor volume ~200 mm^3. ANOVA determined no statistically significant difference among the mean starting tumor volumes of the study groups. MLN2704 and other test articles were administered through injection into the tail vein. Time taken for tumors

Received 5/18/04; revised 8/14/04; accepted 9/10/04.

The costs of publication of this article were defrayed in part by the payment of page charges. This article must therefore be hereby marked *advertisement* in accordance with 18 U.S.C. Section 1734 solely to indicate this fact.

Note: Authors are either former (M. Henry) or current (S. Wen, M. Silva, S. Chandra, M. Milton, P. Worland) employees of and currently own stock and/or stock options in Millennium Pharmaceuticals, Inc.; M. Henry is currently in the Department of Physiology and Biophysics, Carver College of Medicine, University of Iowa, Iowa City, Iowa; supplementary data for this article can be found at Cancer Research Online (http://cancerres.aacrjournals.org).

Requests for reprints: Peter Worland, Millennium Pharmaceuticals, Inc., 40 Landsdowne Street, Cambridge, MA 02139. E-mail: peter.worland@mpi.com.

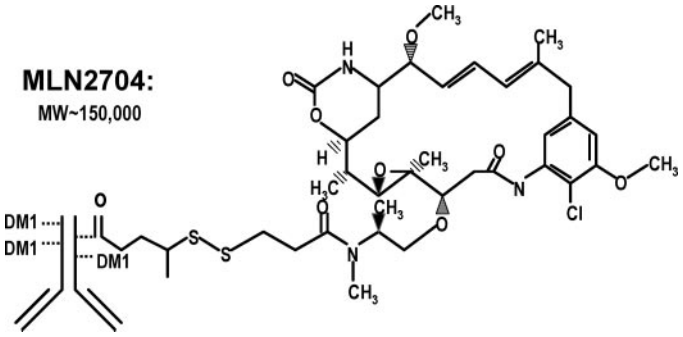

Fig. 1. Schematic of MLN2704. *MW*, molecular weight.

to reach 1,000 mm^3 ($t_{1000mm3}$) was calculated by graphical analysis of tumor growth curves. Tumor growth delay was calculated by $t_{1000mm3}$ (treatment group) − $t_{1000mm3}$ (PBS group). For the intraosseous tumor model, 22 Rv1 cells (American Type Culture Collection, Manassas, VA) were cotransfected with a luciferase expression vector [pGL3-luc (Promega, Madison, WI)] and a neomycin resistance cassette. Neomycin-resistant clones were screened for luciferase expression. Luciferase-expressing 22Rv1 cells were then screened for PSMA expression by Western blot analysis and were tested for sensitivity to MLN2704 *in vitro* with a tetrazolium dye assay (Roche Applied Science, Indianapolis, IN). One clone, 22Rv1luc#1.17, was selected for *in vivo* model development. Male *scid* mice were anesthetized, and a small hole was drilled in the surgically exposed right tibia. Approximately 1.5×10^5 22Rv1luc#1.17 cells were injected into the bone marrow cavity with a 30-gauge needle and Hamilton syringe. After injection, the hole was sealed with bone wax, and the incision was closed with wound clips. For bioluminescence imaging, animals were given injections intraperitoneally with 100 μL luciferin (15 mg/mL in PBS) per 10 g of body weight. After injection, animals were anesthetized by isoflurane inhalation and were maintained on 1- to 3-% isoflurane in oxygen delivered through nose cones on a manifold in an IVIS (Xenogen, Alameda, CA). Data analysis was performed with Xenogen Living Image software. μCT (micro-computed tomography) imaging was performed on a Scanco Medical μCT-40 (Scanco Medical AG, Zurich, Switzerland). The excised mouse legs were secured in imaging tubes and scanned with the following settings: 30 μm × 30 μm × 31 μm resolution (30. 72 mm × 30. 72 mm × 5.5-to-8 mm field-of-view, 1024 × 1024 × 180-to-260 data matrix), 150 ms X-ray exposure (integration) time (55 kVp and 145 μA), and 1000 projections. Total imaging time was ~1 hour per sample. Image analysis and display was performed with Analyze 4.0 (AnalyzeDirect Inc., Lenexa, KS).

Pharmacokinetic Study. We prepared male, 5- to 8-week-old C.B-17 *scid* mice bearing CWR22 tumors as described above. The mice were randomized into groups (three mice per time point). MLN2704 was administered intravenously via a lateral tail vein. Mice were euthanized by CO_2 inhalation, and blood was collected by cardiac puncture and placed into a tube containing lithium heparin. Blood samples collected from three mice at 0 (predose), 1, 4, 8, 24, 48, 96, 168, 240, and 336 hours postdose, were centrifuged, and the plasma was stored at approximately −80°C until analysis. The concentrations of the conjugated antibody MLN2704, the deconjugated antibody (free MLN591; consisting of MLN591 plus the remainder of the thiopentanoate linkages) and total antibody-related material (total MLN591) were measured by specific ELISA methods. To quantify total MLN591, the wells of a microtiter plate were coated with 100 μL of an anti-MLN591 antibody; the plates were incubated at room temperature 60–120 minutes and then were washed and blocked with 150 μL of 5% nonfat dry milk in PBS. Plates were incubated at room temperature for ~60 minutes and were washed, and 100 μL of unknown sample (diluted to fall in the linear range of the standard curve) were added. An incubation for 60 minute at room temperature was done before washing and before the addition of 100 μL of secondary antibody (mouse anti-human IgG-horseradish peroxidase), and then the plate was incubated at room temperature for ~60 minutes. Finally, after washing the plate, 100 μL of colorimetric substrate were added and the mixture was incubated for 15 to 30 minutes before measuring the absorbance of the wells at 650 nm. From this data, we constructed a standard curve and calculated the concentrations of MLN591. For MLN2704 quantitation, the methods were similar to those described above, except that microtiter plate wells were coated with 100 μL of an anti-DM1 antibody. The method to quantitate free MLN591 required a sample pretreatment step in which we separated MLN2704 from free MLN591 (deconjugated antibody) by incubating the sample in an anti-DM1-coated microtiter plate. The supernatant containing free MLN591 was assayed as for total MLN591 described above.

Western Blot and Immunofluorescence Analysis. For Western blot analysis, cell pellets or tumor cryosections were resuspended in 100 μL of lysis buffer containing 1% NP40, 150 mmol/L NaCl, 50 mmol/L HEPES (pH 7.5), 2 mmol/L EDTA, 5% glycerol, and both 1 mmol/L DTT and 1X protease inhibitor cocktail (Roche Applied Science) were added immediately before use. Proteins (loaded at 10 μg per lane) were resolved by SDS-PAGE with 10% Tris-glycine gels and electrophoretically transferred to nitrocellulose with Tris glycine transfer buffer. For immunofluorescence analysis, freshly isolated tumor tissue collected from mice in study groups was embedded and flash-frozen in liquid nitrogen. Sections were fixed, blocked, and stained with MLN591. Stained sections were washed, incubated in secondary antibody solution (anti-Human Alexa fluor (Molecular Probes, Eugene, OR), washed again, and mounted on slides.

RESULTS

The pharmacokinetics of MLN2704 was determined in *scid* mice bearing CWR22 xenografts. Because MLN2704 comprises of an antibody moiety (MLN591) and DM1 coupled by a labile disulfide

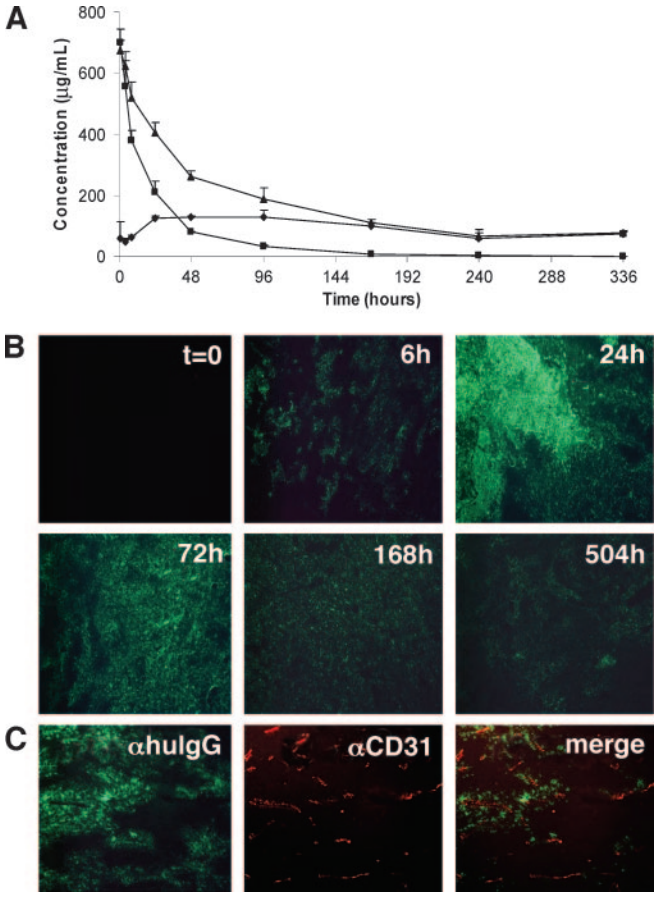

Fig. 2. Pharmacokinetics and tumor distribution of MLN2704. *A*, plasma concentration *versus* time curves for MLN2704 (■), free MLN591 (♦), and total MLN591 (▲). *B*, fluorescent micrographs of representative sections of CWR22 tumor tissue stained to detect the human IgG (*huIgG*) component of MLN2704 at various times in hours ((*h*; *t=0, 6h*, *24h*, and so forth) after the administration of a single bolus intravenous dose of MLN2704 at a level of 240 μg DM1 equivalents per kg. *C*, double-label immunofluorescence micrographs from sections of CWR22 tumors 24 hours postdose with 240 μg DM1 equivalents per kg showing human IgG (*green*) and anti-CD31 (*red*) vascular staining.

Table 1 *Mean pharmacokinetic parameters of MLN2704, total MLN591, and free MLN591*

Analyte	T_{max} (h)	C_{max} (μg/mL)	*AUC* 0–336 h (μg*h/mL)	$T_{1/2}$ (h)	*CL* (mL/h/kg)	*Vss* (mL/kg)	*Vz* (mL/kg)
Total MLN591	1	676	55400	99.9	0.901	122	130
MLN2704	1	701	17200	39.2	3.48	151	197
Free MLN591*	48	128	31200	268	1.01	NC	391

Abbreviations: T_{max}, time to maximum plasma concentration; C_{max}, maximum plasma concentration; *AUC* 0–336 h, area under time-concentration curve; $T_{1/2}$, terminal phase half-life; CL, plasma clearance; Vss, volume of distribution at steady state;Vz, volume of distribution associated with terminal phase; NC, not calculated.

* CL and Vz for free MLN591 are Vz/F. However, for an intravenous injection, F is assumed to be equal to 1.

linkage, specific analytical methods were developed to quantify total MLN591 (conjugated and deconjugated antibody), MLN2704 (conjugated antibody), and free MLN591 (deconjugated antibody). MLN2704 and total MLN591 plasma concentrations seemed to decline in a biphasic manner (Fig. 2*A*, Table 1) with similar maximal concentrations of total MLN591 and MLN2704 (676 and 701 μg/mL, respectively) observed at the earliest sampling time point (1 hour postdose). MLN2704 was cleared more rapidly than was free MLN591 (3.48 mL/h/kg and 1.01 mL/h/kg, respectively) and with a shorter plasma half life of almost 40 hours compared with an estimated half-life of 268 hours for the free MLN591 (see Table 1). Consequently, by 48 hours, the plasma concentrations of MLN591 were greater than for MLN2704. On the basis of the AUC estimates, approximately one third of the exposure to circulating administered antibody was in the form of MLN2704. The volume of distribution at steady state (V_{ss}) for MLN2704 was 151 mL/kg.

The distribution of the MLN591 component of MLN2704 in CWR22 xenografts was determined, after the dosing of tumor-bearing animals with MLN2704 (240 μg DM1 equivalents per kg), by analysis of isolated tumor tissue at defined time points postdose. Tumor sections were stained with fluorescently labeled anti-human IgG antibodies to detect MLN591 (Fig. 2*B*). Six hours postdose, the MLN591 distribution within CWR22 tumors was highly heterogeneous. Colabeling with anti-CD31 revealed that the initial MLN591 distribution was highly correlated with the CD31-positive blood vessels, consistent with vascular delivery of MLN2704 to the CWR22 tumor (Fig. 2*C*). The staining appeared most intense at 24 hours postdose, but at this time, there remained regions with less-intense-to-undetectable staining for MLN591. At later time points, the distribution appeared more homogeneous, although reduced in the staining intensity. Some isolated pockets of tumor cells were negative for staining. The specific staining signal was noted up to 21 days postdose when human IgG signal was detectable above background for some regions of the tumor. This experiment indicated that MLN591 enters CWR22 tumors through the vasculature and distributes throughout the tumor, almost homogeneously, within 3 days postdose. However, it is currently not possible to determine what fraction of the detectable MLN591 is present as unconjugated or DM1-conjugated species.

The PSMA-positive CWR22 prostate cancer xenograft model was used to evaluate the *in vivo* efficacy of MLN2704 and to make a comparison with its constituent elements, MLN591 and DM1. MLN2704, MLN591, and DM1 were administered on a one-dose-every-3-days-for-five-doses (q3d×5) schedule at equivalent intravenous bolus doses calculated for either antibody (12.93 mg/kg) or DM1 (240 μg/kg), previously defined as the maximum tolerated MLN2704 dose level on an every-day-for-5-days (qd×5) schedule (data not shown). MLN2704 treatment exhibits a more potent tumor-growth-delay effect than does either of its constituents (Fig. 3*A*; Table 2). At a dose level of 240 μg of DM1 equivalents per kg on a q3d×5 schedule, MLN2704 resulted in a tumor growth delay of 46.4 days compared with DM1 (tumor growth delay of 9.5 days; $P = 0.006$) and MLN591 (tumor growth delay of 1.9 days), which was not significantly different from that with vehicle control. MLN2704 efficacy was dose dependent, because lower doses, 90, 120, or 180 μg/kg, produced correspondingly shorter tumor growth delays of 31.9, 37.8, and 42.7 days, respectively. Dependence on PSMA expression for the efficacy of MLN2704 was determined by comparing a humanized monoclonal antibody conjugate that does not react with CWR22 tumor cells, anti-human CCR2-DM1 (Fig. 3*B*; Table 2), administered at the same dose and schedule [every 7 days for five doses (q7d×5); 240 μg DM1 equivalents per kg]. MLN2704 treatment yielded a tumor growth delay of 55.2 days, whereas anti-human CCR2-DM1 yielded only a minor tumor growth delay of 3.7 days. MLN2704 did not exhibit any overt toxicity, as judged by mortality or body weight loss of >15%, during the dosing regimen at any of the doses and schedules evaluated in this study (Table 2). Although MLN2704 effected remarkable tumor growth delay, cures were not observed in the CWR22 xenograft because, after the cessation of treatment, tumors eventually resumed growth. However, CWR22 tumors, exhibiting regrowth after cessation of a first course of MLN2704 treatment, continued to express PSMA, and those tumors will respond to a second course of treatment (Supplemental data).[4] These results demonstrate that MLN2704 delivers a substantially more potent tumor growth delay effect in the CWR22 xenograft than does either of its constituent elements alone or a nonreactive monoclonal antibody-DM1 conjugate.

Prior experiments had suggested that increasing dosage intervals would produce a greater tumor growth delay (compare q3d×5 or q7d×5 schedules, Figs. 3*A* and *B* and Supporting Information).[4] This was explored more fully by comparing tumor growth delay for every-7-day, every-14-day, every-21-day, and every-28-day schedules (Fig. 3*C*; Table 2). Tumor growth delay increased as dosage interval increased from 7 days to 14 days, but then began to decrease as dosage interval increased from 14 days to 21 days and 28 days. The shape of the tumor growth curves suggests a slowing of the tumor growth rate for every-21-days or every-28-days, when, in contrast, at the every-3-day, every-7-day, and every-14-day intervals, tumor volume remained static throughout the treatment period and resumed growth only at some point after the cessation of treatment (see Fig. 3). Having determined the optimal schedule of every-14-days in the CWR22 model, we compared a range of doses at this interval (Fig. 3*D*). At all of the dosage levels tested on the one-dose-every-14-days-for-five-doses (q14d×5) schedule, there was no evidence of overt toxicity (Table 2); and at the maximum dose tested (60 mg/kg), five of seven tumors regressed and were not palpable at the end of the treatment period, day 56. However, these tumors eventually resumed growth after a considerable delay (~100 days). Thus, the maximum tumor growth delay effect of MLN2704 requires both an optimized dosage and an optimized dose schedule.

A novel model of prostate cancer bone metastasis was developed to further evaluate the efficacy of MLN2704. The 22Rv1 prostate cancer cell line was transfected to express firefly luciferase, and luciferase-expressing clones were screened for PSMA expression by Western blot analysis. Several luciferase-expressing clones were isolated that

[4] Supplementary data for this article can be found at Cancer Research Online (http://cancerres.aacrjournals.org).

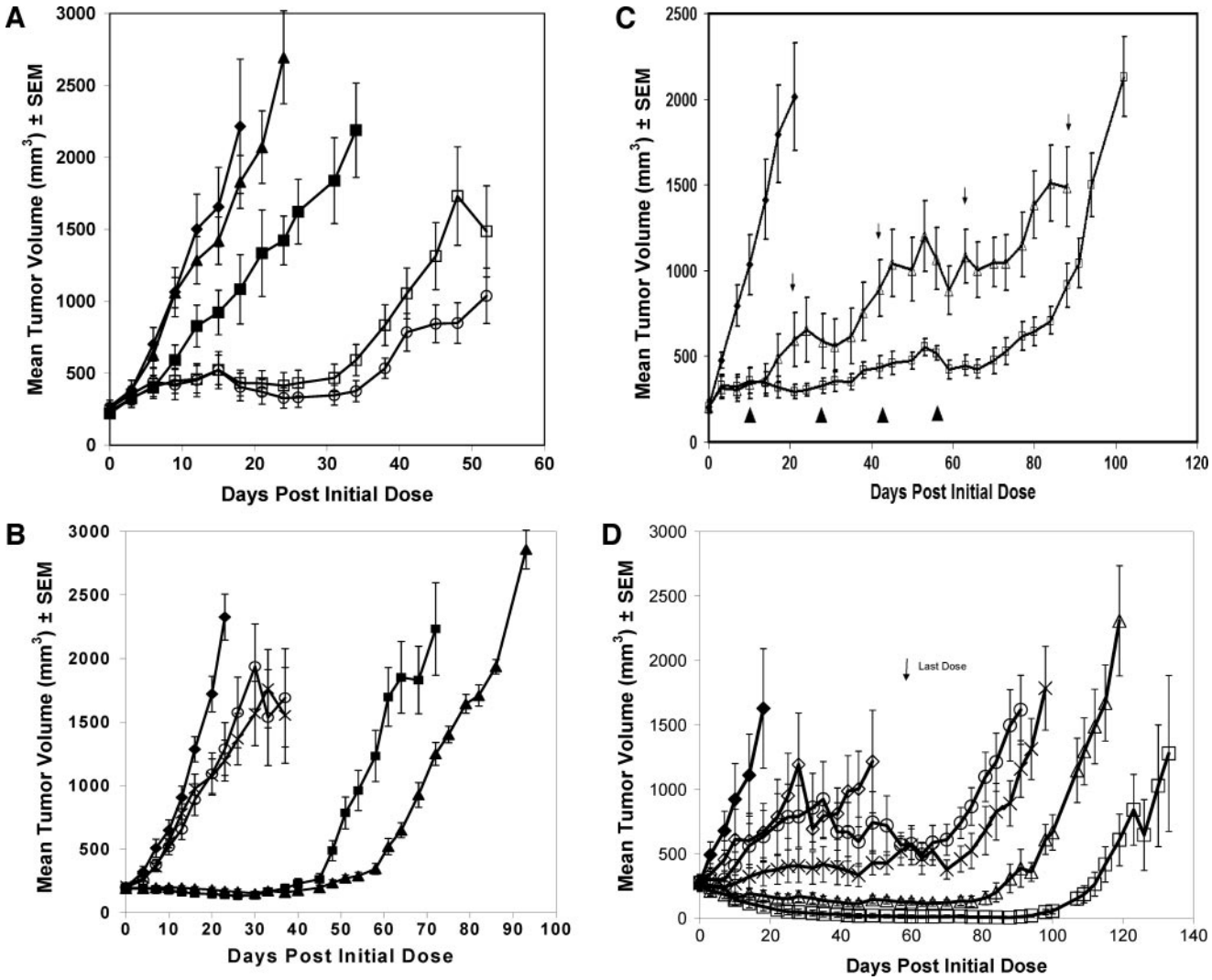

Fig. 3. MLN2704 exhibits potent and specific antitumor efficacy in a dose- and schedule-dependent manner. *A*, CWR22 tumor growth curves during and after treatment every 3 days for 5 doses of PBS, (♦); and of MLN591, 12.96 mg/kg (▲); DM1, 240 μg/kg (■); MLN2704, 90 μg DM1 equivalents/kg (□); and 240 μg DM1 equivalents/kg (○). *B*, CWR22 tumor growth curves during and after treatment with five doses of PBS every 3 days (♦); of MLN2704, 240 μg DM1 equivalents/kg, every 3 days (■) and every 7 days (▲); and of anti-human CCR2-DM1, 240 μg DM1 equivalents/kg, every 3 days (×) and every 7 days (○). *C*, CWR22 tumor growth curves during and after treatment with five doses of PBS every 7 days (♦); and of MLN2704, 240 μg DM1 equivalents/kg, every 14 days (□) and every 21 days (△). *Arrowheads*, dose administration on the every-14-day schedule; *arrows*, dose administration on the every-21-day schedule. *D*, CWR22 tumor growth curves during and after treatment every 14 days for 5 doses of PBS (♦); and of MLN2704, 5 mg/kg (◇), 10 mg/kg (○), 15 mg/kg (×), 30 mg/kg (△), and 60 mg/kg (□).

expressed various amounts of PSMA (Fig. 4*A*). These were tested forsensitivity to MLN2704 *in vitro*. MLN2704 potency was correlated with PSMA expression level (Fig. 4*B*), and the most sensitive clone 22Rv1luc#1.17 (EC_{50}, ~1 nmol/L) was chosen for *in vivo* model development. For the bone metastasis model, 22Rv1luc#1.17 cells were injected directly into the tibiae of *scid* mice and ~2 weeks were allowed for the tumor to establish; tumor growth was monitored by bioluminescence imaging with a Xenogen IVIS (Fig. 4*C*). MLN2704 treatment (q3d×5; 15 mg/kg) resulted in substantial tumor growth inhibition, whereas anti-human CCR2-DM1 at an equivalent dose had no effect. At 47 days after the initiation of treatment (34 days after the final dose), the tumors in mice receiving MLN2704 displayed only 20% of the bioluminescent signal of control mice. We examined bone morphology in our model by μCT imaging (Fig. 4*D*). In control animals, 22Rv1 tumor growth elicited a mixed osteoblastic/osteolytic response as evidenced by radial spicules emanating from the tibia, as well as erosion of the tibia. In MLN2704-treated animals, there was little or no evidence of osteoblastic response and a reduction in the amount of bone erosion.

DISCUSSION

We have demonstrated that MLN2704 delivers potent, dose-dependent antitumor efficacy at nontoxic dose levels in animal models of prostate cancer. MLN2704 activity requires specific antibody-dependent targeting of DM1 to a PSMA-expressing tumor. MLN2704 was demonstrated as ~5-fold more effective than an equivalent amount of DM1 administered on the same dosage schedule, and, with this same regimen, the unconjugated antibody alone was ineffective. The efficacy of MLN2704 is not simply due to the antibody moiety altering the pharmacokinetic properties of DM1 because the anti-human CCR2-DM1 conjugate failed to produce a significant efficacious response. When MLN2704 was tested over a large dosage range, it was nontoxic up to the highest dose (60 mg/kg; >1 mg DM1 equivalents per kg) tested in these studies, based on the parameters of body weight loss and mortality. A single dose of 1 mg/kg of maytansine is toxic in *scid* mice (data not shown). MLN2704 fulfills the criteria for an ideal immunoconjugate in this preclinical model, possessing significantly enhanced antitumor activity through antigen-dependent tar-

Table 2 *CWR22 tumor growth delay (TGD) in MLN2704 efficacy studies*

Study and test articles	Dose DM1 eq. (mg/kg)	Dose (mg/kg)	Schedule	Day of final dose	$t_{1000mm3}$ (d * ± SEM)	TGD (d) †	ΔBW (%) †
Fig. 3*A*							
PBS	NA	NA	q3d×5	12	8.1 ± 1.3	NA	0
DM1	240	NA	q3d×5	12	17.6 ± 2.3	9.5	−6.5
MLN591	NA	13.0	q3d×5	12	10.0 ± 1.7	1.9	+1.6
MLN2704	90	4.8	q3d×5	12	40.0 ± 2.0	31.9	−1.6
MLN2704 ‡	120	6.5	q3d×5	12	45.9 ± 2.7	37.8	−2.8
MLN2704 ‡	180	9.7	q3d×5	12	50.8 ± 2.7	42.7	+1.2
MLN2704	240	12.9	q3d×5	12	54.5 ± 4.6	46.4	−2.4
MLN2704 ‡	120	6.5	q7d×5	28	42.0 ± 6.6	33.9	−10.4
MLN2704 ‡	240	12.9	q7d×5	28	74.9 ± 4.9	66.8	−6.0
Fig. 3*B*							
PBS	NA	NA	q3d×5	12	13.7 ± 0.9	NA	−3.6
MLN2704	240	12.9	q3d×5	12	56.1 ± 2.7	42.4	−1.6
MLN2704	240	12.9	q7d×5	28	68.9 ± 1.0	55.2	+2.0
αCCR2-DM1	240	10.4	q3d×5	12	15.2 ± 1.1	1.5	−3.6
αCCR2-DM1	240	10.4	q7d×5	28	17.4 ± 1.7	3.7	+3.6
Fig. 3*C*							
PBS	NA	NA	q7d×5	28	11.4 ± 2.0	NA	−1.2
MLN2704 ‡	240	12.9	q7d×5	28	64.4 ± 4.9	53.0	−1.2
MLN2704	240	12.9	q14d×5	56	87.1 ± 2.2	75.7	−2.0
MLN2704	240	12.9	q21d×5	84	59.4 ± 8.9	48.0	−9.1
MLN2704 ‡	240	12.9	q28d×5	112	38.3 ± 4.5	26.9	−2.2
Fig. 3*D*							
PBS	NA	NA	q14d×5	56	14.5 ± 3.1	NA	+1.5
MLN2704	89	5	q14d×5	56	23.3 ± 7.5	8.8	−10.8
MLN2704	179	10	q14d×5	56	48.7 ± 13.3	33.2	−7.6
MLN2704	268	15	q14d×5	56	72.7 ± 9.5	58.2	−5.4
MLN2704	536	30	q14d×5	56	100.8 ± 3.0	86.3	+8.4
MLN2704	1060	60	q14d×5	56	122.4 ± 3.2	107.9	+5.6

Abbreviations: eq., equivalent; $t_{1000mm3}$, mean time to reach tumor volume of 1000mm^3; ΔBW, percent change in body weight from time of initial dose to final dose; NA, not applicable; q3d×5, every 3 days for five doses; q7d×5, every 7 days for five doses; q14d×5, every 14 days for five doses; q21d×5, every 21 days for five doses; q28d×5, every 28 days for five doses.

† See Materials and Methods for a description of how these values were calculated.

‡ For graphical clarity, these groups were omitted from Fig. 3.

geting of a chemotherapeutic agent and reduced toxicity by limited systemic exposure of the cytotoxic moiety.

Pharmacokinetic analyses showed that MLN2704 was cleared from the plasma with a concomitant time-dependent appearance of free MLN591. The rate of MLN2704 clearance was approximately three times higher than for free MLN591, which showed pharmacokinetics that were similar to other human IgGs evaluated in *scid* mice (14). Cantuzumab mertansine, another DM1 containing immunoconjugate has been previously observed to be cleared more rapidly than total antibody-related material in humans and in mice (15, 16). Like MLN2704, this agent uses a sulfhydryl linker system designed to release the DM1 after internalization to the PSMA-expressing tumor cells. However, we have not defined in which compartment(s) the deconjugation occurs. It is possible that compartments in addition to the tumor will contribute to this process of deconjugation and, hence, the clearance of MLN2704. Regardless, adequate levels of MLN2704 are maintained in the plasma and tumor tissue sufficient for tumor cell killing based on levels of MLN2704 necessary for cytotoxic effects *in vitro* (~1 nmol/L). Moreover, the efficacy observed after MLN2704 administration indicates superior delivery of the cytotoxic DM1 to the site of action, when compared with the efficacy after administration of either MLN591 or DM1 alone. By immunofluorescence analysis, we showed that the antibody MLN591 was detectable penetrating into the CWR22 xenograft tissue and was almost uniformly distributed by 72 hours. Although we have not assessed the extent to which DM1 is still present on this antibody, this experiment considered with the pharmacokinetic analysis and efficacy data suggests that MLN2704 distributes well into tumor tissue, exposing PSMA-expressing tumor cells to cytotoxic levels of drug.

The appearance of free MLN591 antibody raises a question regarding potential competitive inhibition with MLN2704 at the site of action. This will depend on the degree of saturation of tumoral antibody uptake mechanisms, PSMA receptor binding, and resultant relative ratios of MLN591 and MLN2704 in the tumor microenvironment. Because PSMA is such a highly abundant receptor on the surface of prostate cancer cells, receptor saturation at the dose levels used seems unlikely (17). Indeed, the murine monoclonal antibody that MLN591 is based on, J591, conjugated to ricin, shows *in vitro* efficacy at concentrations far below those required for receptor saturation (18). Furthermore, our own *in vitro* studies show similar results for MLN2704 and that anti-CWR22 tumor efficacy *in vivo* was not substantially blocked when coadministered with an equimolar dose of MLN591 (data not shown). From the pharmacokinetic analysis, MLN591 will achieve higher concentrations than MLN2704 after ~48 hours. At several dosages and schedules out to every-14-days (q14d), an efficacious response was observed, which indicated that the circulating MLN591 produced by the given doses does not prevent the tumor growth-inhibitory activity of MLN2704. In fact, increasing the dosage to 30 or 60 mg/kg on the q14d schedule, which would produce plasma concentrations of MLN591 in the tens of nanomolar range, does not diminish the efficacy of MLN2704. Moreover, the antibody moiety may engage immune responses that would contribute to efficacy in patients, which cannot be measured in the immunocompromised mouse models studied here.

MLN2704 antitumor efficacy exhibited strong schedule dependency. For the CWR22 xenograft model, efficacy was maximized when administered once every 2 weeks. At equivalent dosage levels, the observed efficacy on the 2-week schedule was as much as three times greater than on either shorter or longer dosage intervals. However, if the tumor growth delay is calculated from the time of last administered dose, for schedules from every day to q14d, it is quite informative to find that they are within the range of 34 to 39 days regardless of schedule. This strongly suggests that, at this dose we can maximize duration of response by increasing the interval to 14 days, which is an interval before the tumor can recover and resume growth. In contrast, increasing the interval to 21 days extends the schedule to the point at

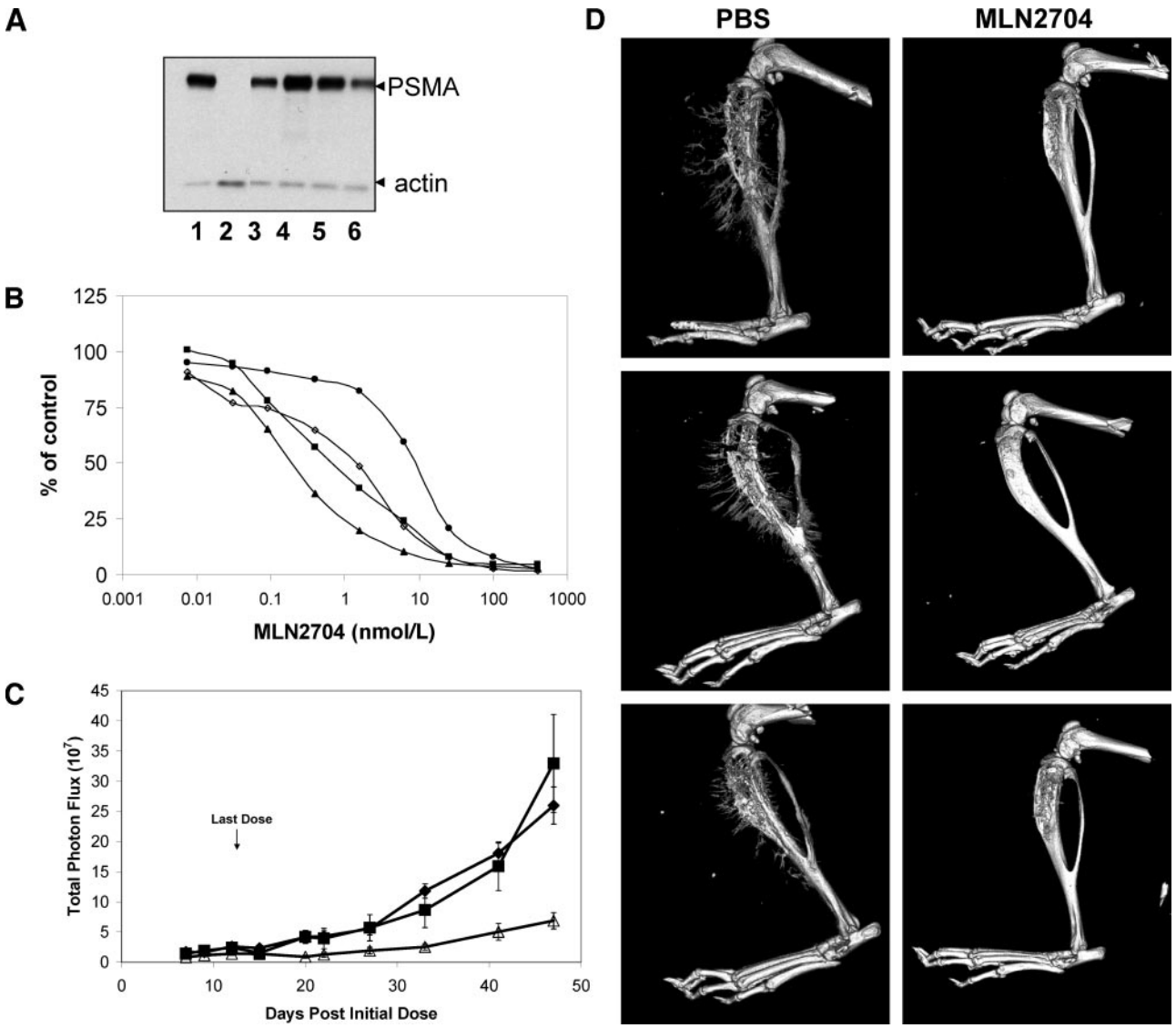

Fig. 4. MLN2704 inhibits tumor growth in a model of osteoblastic prostate cancer metastasis. A, PSMA expression: *Lane 1*, LNCaP; *Lane 2*, PC3; *Lane 3*, 22Rv1 (parental); *Lane 4*, 22Rv1luc#1.17; *Lane 5*, 22Rv1luc#1.3; *Lane 6*, 22Rv1luc#1.5. *B*, cytotoxic effect of MLN2704 in LNCaP (◇), 22Rv1luc#1.17 (▲), 22Rv1luc#1.3 (■), and 22Rv1luc#1.5 (●) cells. *C*, bioluminescence imaging of 22Rv1luc#1.17 intraosseus tumor growth in mice treated every 3 days for 5 doses with PBS (♦); with MLN2704 240 μg DM1 equivalents/kg (△); and with anti-human CCR2-DM1 240 μg DM1 equivalents/kg (■). *D*, representative μCT scans obtained from PBS (every 3 days for 5 doses) and MLN2704 (240 μg DM1 equivalents/kg, every 3 days for 5 doses) treatment groups.

which the control of tumor growth is observed for several days, but before the next dose, tumor growth resumes (Fig. 3*C*). With the pharmacokinetic data, a relationship between plasma concentrations of MLN2704 and tumor growth control can be proposed that would suggest that, at higher doses, increased dosage intervals may be efficacious.

We did not observe cures by MLN2704 treatment in our models. Even at the highest dose levels tested, after dramatically regressing, tumors eventually grew back with a tumor growth delay of ~100 days. However, resumed tumor growth was not due to an acquired resistance to MLN2704, because tumors remained sensitive to a second course of treatment and expressed a similar amount of PSMA compared with untreated tumors. In the present series of experiments, each study was restricted to five cycles of treatment, but it would appear that continued treatment with MLN2704 may be necessary to ultimately result in a "cure" for the CWR22 xenograft. This result argues for continued treatment to maximize antitumor effect.

Approximately 65 to 75% of prostate cancer patients will develop bone metastasis during the course of their disease (19). A novel model of osteoblastic bone metastasis, created by injecting luciferase-expressing 22RV1 cells into the tibiae of *scid* mice was used to demonstrate that MLN2704 is effective against the tumor growth in this setting. Over the course of 7 weeks, untreated tumors grew and exhibited features of osteoblastic bone metastasis. MLN2704 treatment blocked both tumor growth in this model and the elaboration of osteoblastic lesions. We are currently investigating the features of this model to determine how well it represents clinical prostate cancer metastasis. Activity in this model is particularly encouraging with respect to its potential clinical application and incidence of bone metastasis from prostate cancer.

MLN2704 is just one of several therapeutic modalities based on the MLN591 (huJ591) antibody currently being evaluated in the clinic. Phase I clinical trials testing the MLN591 (huJ591) antibody alone, in combination with interleukin-2 and as a radioconjugate, have been completed or are ongoing, the latter (that is, in combination with radioconjugate) having demonstrated evidence of preclinical antitumor activity (20, 21). Other studies have demonstrated that the murine monoclonal antibody J591, on which MLN591 is based, can effec-

tively target bone metastases in prostate cancer patients, based on imaging analysis (22). Our studies are the first that demonstrate the antitumor activity of a MLN591-based therapeutic in an animal model of prostate cancer metastasis. Present clinical studies will determine whether these results will translate into activity of MLN2704 against bone metastases in the clinic and offer these patients a much needed treatment option in this area of critical unmet medical need.

ACKNOWLEDGMENTS

The authors gratefully acknowledge Dr. Thomas Pretlow (Case Western Reserve University, Cleveland, OH) for the CWR22 xenograft; William Riordan and Marie Green for development of analytical ELISA assays; the Millennium CMC group, Molly Myers, Jihee Im, Elina Tang, Greg Papastoitsis, Jessica Riceberg, and Anne Burkhardt for advice and technical assistance; and Gary Gray, Ian Webb, and Joe Bolen for critical reading of the manuscript.

REFERENCES

1. Payne G. Progress in immunoconjugate cancer therapeutics. Cancer Cell 2003;3:207–12.
2. Tasch J, Gong M, Sadelain M, Heston WD. A unique folate hydrolase, prostate-specific membrane antigen (PSMA): a target for immunotherapy? Crit Rev Immunol 2001;21:249–61.
3. Schulke N, Varlamova OA, Donovan GP et al. The homodimer of prostate-specific membrane antigen is a functional target for cancer therapy. Proc Natl Acad Sci 2003;100:12590–5.
4. Israeli RS, Powell CT, Corr JG, Fair WR, Heston WD. Expression of the prostate specific membrane antigen. Cancer Res 1994;54:1807–11.
5. Bostwick DG, Pacelli A, Blute M, Roche P, Murphy GP. Prostate specific membrane antigen expression in prostatic intraepithelial neoplasia and adenocarcinoma: a study of 184 cases. Cancer (Phila) 1998;82:2256–61.
6. Liu H, Moy P, Kim S, et al. Monoclonal antibodies to the extracellular domain of prostate specific membrane antigen also react with tumor vascular endothelium. Cancer Res 1997;57:3629–34.
7. Liu H, Rajasekaran AK, Moy P et al. Constitutive and antibody-induced internalization of prostate specific membrane antigen. Cancer Res 1998;58:4055–60.
8. Gong MC, Chang SS, Watt F et al. Overview of evolving strategies incorporating prostate specific membrane antigen as target for therapy. Mol Urology 2000;4:217–22.
9. Hamilton A, King S, Liu H, Moy P, Bander N, Carr F. A novel humanized antibody against prostate-specific membrane antigen also reacts with tumor vascular endothelium [abstract]. Proc Am Assoc Cancer Res 1998;39:440.
10. Liu C, Mitra Tadayoni B, Bourret LA et al. Eradication of large colon tumor xenografts by targeted delivery of maytansinoids. Proc Natl Acad Sci USA 1996;93:8618–23.
11. Chari RVJ, Martell BA, Gross JL et al. Immunoconjugates containing novel maytansinoids :promising anticancer drugs. Cancer Res 1992;52:127–31.
12. Blum RH, Wittenberg BK, Canellos GP et al. A therapeutic trial of maytansine. Cancer Clin Trials 1978;1:113–17.
13. Pretlow TG, Wolman SR, Micale MA et al. Xenografts of primary human prostatic carcinoma. J Natl Cancer Inst (Bethesda) 1993;85:394–8.
14. Zuckier LS, Georgescu L, Chang CJ, Scharff MD, Morrison SL. The use of severe combined immunodeficiency mice to study the metabolism of human immunoglobulin G. Cancer (Phila) 1994;73:794–9.
15. Tochler AW, Ochoa L, Hammond LA et al. Cantuzumab mertansine, a maytansinoid immunoconjugate directed to the CanAg antigen: a phase I, pharmacokinetic, and biologic correlative study. J Clin Oncol 2003;21:211–22.
16. Xie H, Audette C, Hoffee M, Lambert JM, Blattler WA. Pharmacokinetics and biodistribution of the antitumor immunoconjugate, cantuzumab mertansine (huC242-DM1), and its two components in mice. J Pharmacol Exp Ther 2004;308:1073–82.
17. Smith-Jones PM, Vallabahajosula S, Goldsmith SJ et al. In vitro characterization of radiolabelled monoclonal antibodies specific for the extracellular domain of prostate-specific membrane antigen. Cancer Res 2000;60:5237–43.
18. Fracasso G, Bellisola G, Cingarlini S et al. Anti-tumor effects of toxins targeted to the prostate specific membrane antigen. Prostate 2002;53:9–23.
19. LoRusso P. Analysis of skeletal-related events in breast cancer and response to therapy. Semin Oncol 2001;28:22–7.
20. Nanus DM, Milowsky MI, Kostakoglu L. et al. Clinical use of monoclonal antibody huJ591 therapy:targeting prostate-specific membrane antigen. J Urol 2003;170:S84–9.
21. Vallabhajosula S, Smith-Jones PM, Navarro V, Goldsmith SJ, Bander NH. Radioimmunotherapy of prostate cancer in human xenografts with monoclonal antibodies specific to prostate specific membrane antigen (PSMA): studies in nude mice. Prostate 2004;58:145–55.
22. Bander NH, Trabulsi EJ, Kostakoglu L. Targeting metastatic prostate cancer with radiolabelled monoclonal antibody J591 to the extracellular domain of prostate specific membrane antigen. J Urol 2003;170:1717–21.

A Prostate-Specific Membrane Antigen-Targeted Monoclonal Antibody–Chemotherapeutic Conjugate Designed for the Treatment of Prostate Cancer

Michael D. Henry, Shenghua Wen, Matthew D. Silva, et al.

Cancer Res 2004;64:7995-8001.